Published in: Thin Solid Film (2010); vol. 518; pp. S18-S22
Authors : Shotaro Takeuchi, Ngoc Duy Nguyen, Jozefien Goosens, Matty Caymax, Roger Loo
Statu : Postprint (Author's version)

$Si_{1-x}Ge_x$ growth using Si_3H_8 by low temperature chemical vapor deposition

Shotaro Takeuchi [a,b,c], Ngoc Duy Nguyen [a], Jozefien Goosens [a], Matty Caymax [a], Roger Loo[a]

[a] *IMEC, Kapeldreef 75, B-3001 Leuven, Belgium*
[b] *Department of Physics and Astronomy, Katholieke Universiteit Leuven, Celestijnenlaan 200D, B-3001 Leuven, Belgium*
[c] *Department of Crystalline Materials Science, Graduate School of Engineering, Nagoya University, Furo-cho, Chikusa-ku, Nagoya 4β4-8β03, Japan*

Keywords: $Si_{1-x}Ge_x$; Si_3H_8;Low temperature; chemical vapor deposition; CMOS;BiCMOS

ABSTRACT: Low temperature epitaxial growth of group-IV alloys is a key process step to realize the advanced Si-based devices. In order to keep high growth rate below 600 °C, trisilane (Si_3H_8) was used for their growth as an alternative Si precursor gas. Then, we compared the use of Si_3H_8 versus SiH_4 for $Si_{1-x}Ge_x$ growth in H_2 and N_2 as carrier gas by low temperature chemical vapor deposition. By using Si_3H_8 and controlling GeH_4 flow rate, $Si_{1-x}Ge_x$ growth with high growth rate and wide range of Ge concentration has been achieved compared to SiH_4-based process. The growth rate and Ge concentration in $Si_{1-x}Ge_x$ with Si_3H_8 grown at 600 °C ranged from 11 to 74nm/min and from 0 to 40%, respectively. The obtained growth rates with Si_3H_8 are between 1.5 and 6 times higher than for SiH_4 at a given growth condition. Si_3H_8-based *in-situ* B- and C-doped $Si_{1-x}Ge_x$ growth with high growth rate was also demonstrated.

1. Introduction

Low-temperature epitaxial growth of group-IV alloys is a key process step for the achievement of advanced Si-based (bipolar) complementary metal-oxide-semiconductor (CMOS, BiCMOS) applications. This process is now used in embedded and raised source/ drains with strained $Si_{1-x}Ge_x$ and strained $Si_{1-y}C_y$ for CMOS and fully-strained base layer of $Si_{1-x}Ge_x$ and $Si_{1-x-y}Ge_xC_y$ for BiCMOS [1-4], Because these Si-based group-IV layers are highly doped and fully-strained, low thermal budget is required to avoid any undesirable dopant diffusion and strain relaxation. For example, it is required to limit the doping diffusion in the *existing* CMOS devices for BiCMOS applications. Obviously, the thermal budget during epi processing is defined by both the pre-epi bake, used to remove traces of oxide and carbon after the last wet-chemical treatment, as well as the growth temperature during epitaxial growth. Several groups (among which IMEC) studied the impact of the pre-epi treatments on substrate/epi interface contamination and its importance for device performance, see for example reference [5,6]. Effort is ongoing to reduce the pre-epi bake temperature to temperatures ≤ the growth temperature. In the classical chemical vapor deposition (CVD) approach, Si-based epitaxial layers were grown by mainly using SiH_4 or $SiCl_2H_2$ as Si precursor gas. A reduction of the growth temperature leads to a large reduction of the growth rate, which means that sustaining a high throughput becomes very difficult. There are two routes to enhance growth rates: one is the use of N_2 as carrier gas instead of H_2 [7]. Another one is the use of high order silane precursor gases such as trisilane (Si_3H_8) [8-10]. High growth rates at growth temperatures below 600 °C for both routes have been demonstrated. However, the growth behavior has not been fully clarified. In this work, we demonstrate $Si_{1-x}Ge_x$ growth using Si_3H_8 (commercially developed by Voltaix as Silcore®) and SiH_4 as Si precursor gases and using either H_2 or N_2 as carrier gas. We will describe the differences of the growth kinetics and behavior for both Si precursor gases and both carrier gases. The success of the developed $Si_{1-x}Ge_x$ process will be illustrated by full Si/SiGe:C base layers which also contain a B doping spike as used in BiCMOS technology. The same layer quality as a conventional process has been achieved but the higher growth rate enables a strong reduction of thermal budget.

2. Experimental

Epitaxial $Si_{1-x}Ge_x$ layer growth was performed in an ASM Epsilon™ 2000 reactor which is a horizontal cold wall, load-locked reduced pressure CVD system. $Si_{1-x}Ge_x$ layer growth between 500 °C and 600 °C was done on 200 mm wafers using GeH_4, (1% diluted in H_2) as Ge precursor gas and the above-mentioned Si precursor gases. B- and C-doped $Si_{1-x}Ge_x$ layer was also grown at 600 °C using 50 ppm B_2H_6 and 1% CH_3SiH_3 diluted in H_2 as B and C source gas, respectively. The focus of this work lies on a reduction of the thermal budget during epitaxial layer growth. Therefore, we used a conventional wet clean and a 2 min pre-epi bake at 1050 °C to remove the native oxide before growth. As mentioned above, the reduction of pre-epi bake temperature is also important and described in [6]. Scanning electron microscopy (SEM) and spectroscopic ellipsometry (SE) were used to measure the $Si_{1-x}Ge_x$ thickness. SE also allows us to extract the Ge concentration. The $Si_{1-x}Ge_x$ surface morphology was inspected by a Nomarski optical microscope and SEM. In order to estimate the crystalline quality of the $Si_{1-x}Ge_x$ layers, photoluminescence (PL) and secondary ion mass spectrometry (SIMS) were used. We also used SIMS to measure the chemical B concentration in our $Si_{1-x}Ge_x$ layers. The resistivity of B-doped $Si_{1-x}Ge_x$ epilayer was calculated by using a classical four-point-probe method combined with the thickness measurement by SE. From this result, the carrier concentration in the epilayer could be estimated from well-known carrier mobility data of Si. As a consequence, our calculated carrier concentration could be overestimated

because the carrier mobility of $Si_{1-x}Ge_x$ in low Ge content region is degraded due to the alloy scattering compared to the carrier mobility of Si [11].

3. Results and discussion

3.1. Crystalline quality of $Si_{1-x}Ge_x$ *using* Si_3H_8

Since Si_3H_8 is a liquid source at room temperature, one of the concerns for the growth of Si_{1-x} Gex using Si_3H_8 is the impurity level in the $Si_{1-x}Ge_x$ layer. Therefore, we first examine the crystalline quality by PL and carbon (C) and oxygen (0) levels in the $Si_{1-x}Ge_x$ layer by SIMS. Fig. 1(a) shows the PL spectra of layer stacks consisting Si-cap (50 nm)/ $Si_{1-x}Ge_x$ (200 nm)/Si(00l) and using SiH_4/H_2 and Si_3H_8/H_2 processes, respectively. Despite of the lower intensity of $Si_{1-x}Ge_x$ with Si_3H_8 compared to the SiH_4 case, high intensity, well-resolved no-phonon (NP) transition and transverse optical (TO) replica from $Si_{1-x}Ge_x$ layer using Si_3H_8 were observed. This illustrates a low defect level and the absence of non-radiative recombination center in the sample. The slightly higher Ge content as confirmed by SE explains the shift of the PL peaks to lower energies for the sample grown with Si_3H_8/ H_2 process. Fig. 1(b) shows the SIMS profile of the same layer stack with Si_3H_8 as shown in Fig. 1 (a). The C and O level in the $Si_{1-x}Ge_x$ layer are below 1 E1 8 at/cm^3. This impurity level is similar to that of SiH_4-based process. These results indicate good crystalline and interface quality of $Si_{1-x}Ge_x$ grown with Si_3H_8.

Fig. *1. (a) PL spectra measured at 77 K of Si-cap (50nm)/ $Si_{1-x}Ge_x$ (200nm)/Si(001). The $Si_{1-x}Ge_x$ was grown using either SiH_4 or Si_3H_8 while the Si-cap was, in both cases, grown with Si_3H_8. The Ge concentrations were 14% for the use of SiH_4 and 16% for the use of Si_3H_s, respectively, as obtained by SE. (b) SIMS profiles of the same sample with Si_3H_8 as shown in Fig. 1 (a). After the well-known surface peaks caused, the C and 0 levels in the $Si_{1\_x}Ge_x$ layer are at the SIMS background levels similar to the SIMS results as obtained for $Si_{1\_x}Ge_x$ layer grown with SiH_4/GeH_4.*

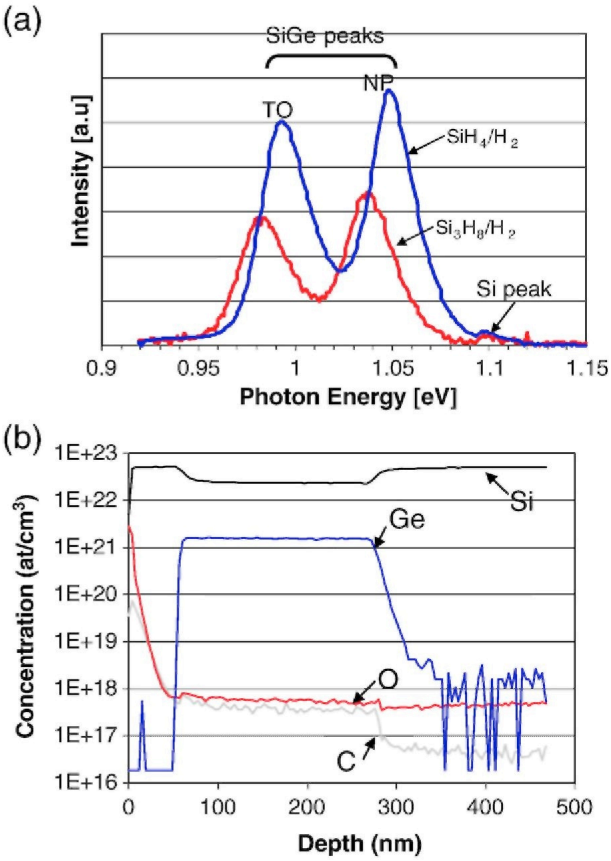

3.2. Comparison of $Si_{1-x}Ge_x$ *growth kinetics with different Si precursor gas and carrier gas*

In the next step, we investigated on the differences between, on the one hand, Si_3H_8 and SiH_4 as Si precursor gas, and, on the other hand, between H_2 and N_2 as carrier gas, regarding the growth behaviors for Si and $Si_{1-x}Ge_x$. In order to perform a fair comparison, the amount of Si atoms injected into the epi reactor is the same for all $Si_{1-x}Ge_x$ growth conditions in this section. Fig. 2's subpanels (a),(b), (c), and (d) show, respectively, the total $Si_{1-x}Ge_x$ growth rates, the Si component deposition rates, the Ge component deposition rates, and the Ge concentrations using SiH_4/H_2, SiH_4/N_2, and Si_3H_8/H_2 processes as a function of the reciprocal temperature. The use of N_2 as a carrier gas or Si_3H_8/H_2 results in a higher growth rate compared to the standard SiH_4/H_2 process (Fig. 2(a)). Generally, at low growth temperature, *i.e.* below 600 °C, the growth rate is controlled by the presence

of H on the growing surface. This H passivation comes from the precursor gases and from the H_2 carrier gas. The low H partial pressure in the SiH_4/N_2 case results then in a higher Si component deposition rate than SiH_4/H_2 case [7]. On the other hand, in the Si_3H_8/H_2 case, although H_2 is used as carrier gas, the Si component deposition rate is much higher than for the SiH_4/H_2 case even at 500 °C (Fig. 2(b)). This means that the adsorption mechanism of Si_3H_8 is different from that of SiH_4 as discussed in the next paragraph. As shown in Fig. 2(c), the Ge incorporation seems to be in the transition region from kinetic to transport regime, especially for the SiH_4/N_2 process. This explains the strong temperature dependence of the Ge content as obtained for the SiH_4/N_2 process (Fig. 2(d)).

Fig. 3(a) and (b) shows $Si_{1-x}Ge_x$ growth rates and Si component deposition rates in the $Si_{1-x}Ge_x$ layer as a function of GeH_4 flow rate, respectively. The growth temperature is fixed at 600 °C Again, the amount of Si atoms injected into the reactor is the same for all $Si_{1-x}Ge_x$ growth conditions. For pure Si growth in H_2 (GeH_4-flow = 0sccm), we obtained higher Si growth rate for Si_3H_8 than for SiH_4. On the other hand, if we use N_2 as carrier gas and GeH_4 flows above 200 sccm, similar $Si_{1-x}Ge_x$ growth rates and Si component deposition rates in the layer are obtained for both Si precursors. Fig. 3(c) shows the normalized Si component deposition rate as function of GeH_4 flow. This rate is defined as [Si component deposition rate in the $Si_{1-x}Ge_x$ layer]/[pure Si growth rate without GeH_4 flow].

The enhancement of the Si component deposition rate by adding GeH_4 called "Ge catalytic effect" [12] is clearly seen in $Si_{1-x}Ge_x$ growth using SiH_4 in H_2. However, for the other three cases, the effect is relatively weak, especially in the case of $Si_{1-x}Ge_x$ growth using Si_3H_8. This is explained by the fact that the Si deposition in the $Si_{1-x}Ge_x$ layer using Si_3H_8 is not limited by hydrogen desorption from the growing surface [14-16]. This can also explain why the Si deposition rate is much higher than for the SiH_4/H_2 case, even at 500 °C A possible explanation for this behavior is that Si_3H_8 can react with a Si-H bound or Si- on the surface forming a four-center bound transition state, due to the nuclephilic character of the Si_2H_5 group, resulting in an "exchange of ligands" with the Si surface (Fig. 4)[14-16]. These Si hydrides with high reactivity decompose to form Si via a facile hydrogen desorption and result in an enhanced $Si_{1-x}Ge_x$ growth rate [13-16]. Similar growth rates are obtained for SiH_4/N_2 and Si_3H_8/N_2 processes (Fig. 3(a)). However, these processes results in defective epilayers, which is not the cases for SiH_4/H_2 and Si_3H_8/H_2 processes.

This growth process needs to be optimized to avoid the generation of defects, which is beyond the scope of this paper.

Fig. 5 shows $Si_{1-x}Ge_x$ growth rates using Si_3H_8 and SiH_4 in H_2 and N_2 as a function of Ge concentration under various growth conditions. The growth rate and the Ge concentration with the SiH_4/H_2 process at 40 Torr range from 0.3 to 21 nm/min and from 0 to 30%, respectively. The incorporation efficiency limits the Ge concentration in the $Si_{1-x}Ge_x$ layer for the Si_3H_8 process. However, it can be solved by an optimization of the process conditions. As shown in Fig. 5, the Si_3H_8/H_2 process provides a high growth rate and a wide variation of Ge concentration in the layer ranging from 11 to 74 nm/min and from 0 to 40% Ge, respectively. For a given Ge concentration in $Si_{1-x}Ge_x$ layer, the use of Si_3H_8/H_2 yields between 1.5 and 6 times higher growth rate than that of SiH_4/H_2.

Published in: Thin Solid Film (2010); vol. 518; pp. S18-S22
Authors : Shotaro Takeuchi, Ngoc Duy Nguyen, Jozefien Goosens, Matty Caymax, Roger Loo
Statu : Postprint (Author's version)

Fig. 2. *(a) $Si_{1-x}Ge_x$ growth rates, (b) Si component deposition rates in the $Si_{1-x}Ge_x$ layer, (c) Ge component deposition rates in the $Si_{1-x}Ge_x$ layer, and (d) Ge concentration using SiH_4/H_2 (blue solid line), SiH_4/N_2 (blue dotted line), and Si_3H_8/H_2 (redsolid line) processes as functions of the reciprocal temperature. $Si_{1-x}Ge_x$ growth temperatures are 500 °C, 550 °C, and 600 °C. The amount of Si atoms injected into the reactor is the same for all growth conditions.*

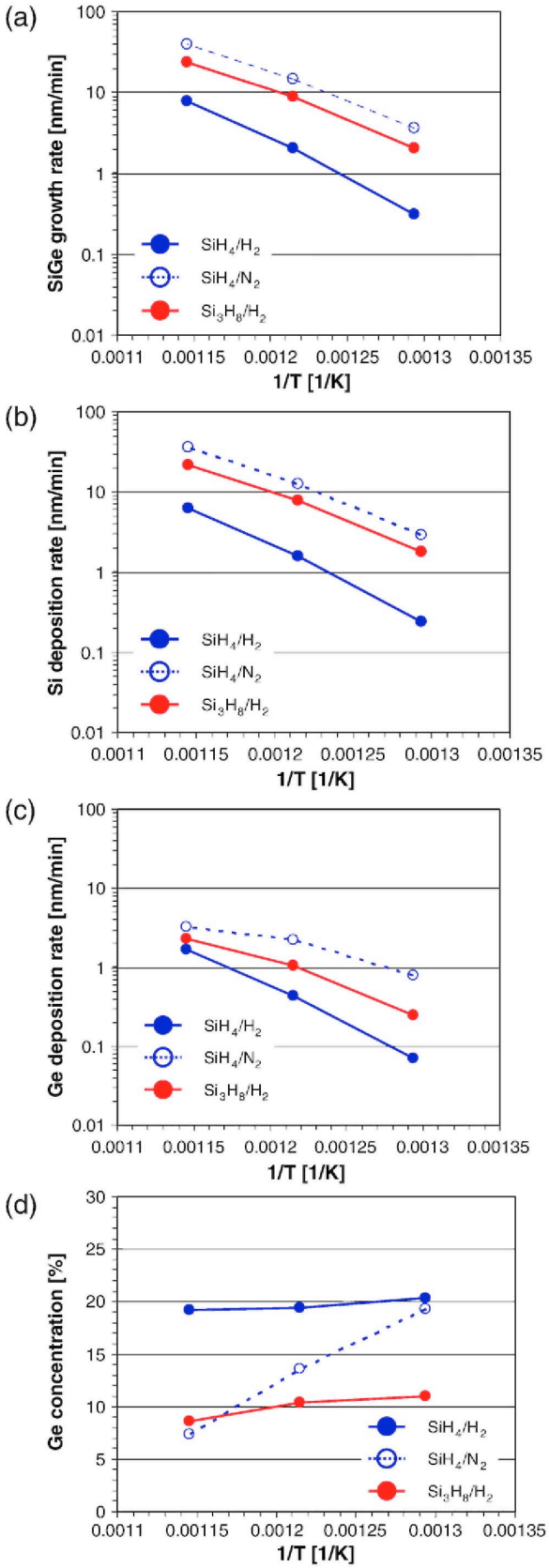

Published in: Thin Solid Film (2010); vol. 518; pp. S18-S22
Authors : Shotaro Takeuchi, Ngoc Duy Nguyen, Jozefien Goosens, Matty Caymax, Roger Loo
Statu : Postprint (Author's version)

Fig. 3. *(a) $Si_{1-x}Ge_x$ growth rates, (b) Si component deposition rate in $Si_{1-x}Ge_x$ layers, and (c) normalized Si component deposition rates using SiH_4/H_2 (blue solid line), SH_4/N_2 (blue dotted line), Si_3H_s/H_2 (red solid line), and Si_3H_s/N_2 (red dotted line) processes as functions of the GeH_4 flow.* $Si_{1-x}Ge_x$ *growth temperature is fixed at 600 °C The amount of Si atoms injected into the reactor is the same for all growth conditions.*

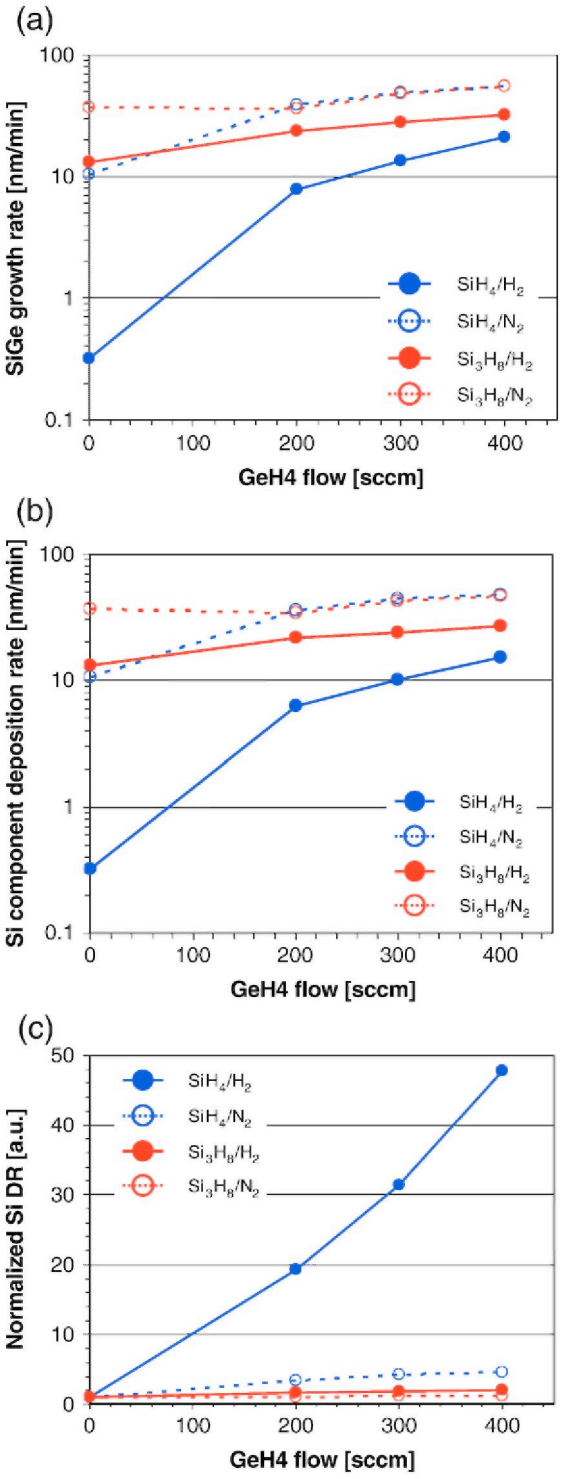

Published in: Thin Solid Film (2010); vol. 518; pp. S18-S22
Authors : Shotaro Takeuchi, Ngoc Duy Nguyen, Jozefien Goosens, Matty Caymax, Roger Loo
Statu : Postprint (Author's version)

***Fig. 4**. Schematic diagrams of a Si_3H_8 dissociation step on a Si site (a) without H passivation, and (b) with H passivation. In both cases, high reactive Si hydrides are generated, leading to an enhancement of the growth rates.*

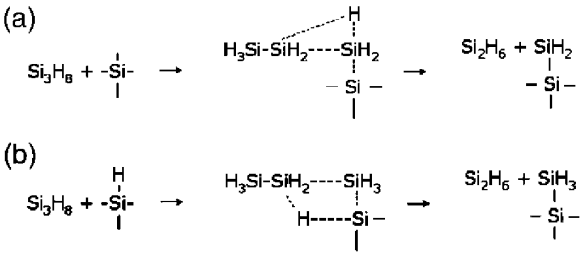

***Fig. 5**. $Si_{1-x}Ge_x$ growth rates as a function of Ge concentration in the layers. Filled blue circles: SiH_4/H_2 process, open blue circles: SiH_4/N_2 process, open red circles: Si_3H_8/N_2 process, $Si_{1-x}Ge_x$ layers are grown at 600 °C and 40 Torr. For Si_3H_s/H_2 process, filled red and pink symbols indicate high and low Si_3H_s flow rate. Triangles: 15 Torr, circles: 40Torr, squares: 80Torr, and diamond: 100Torr.*

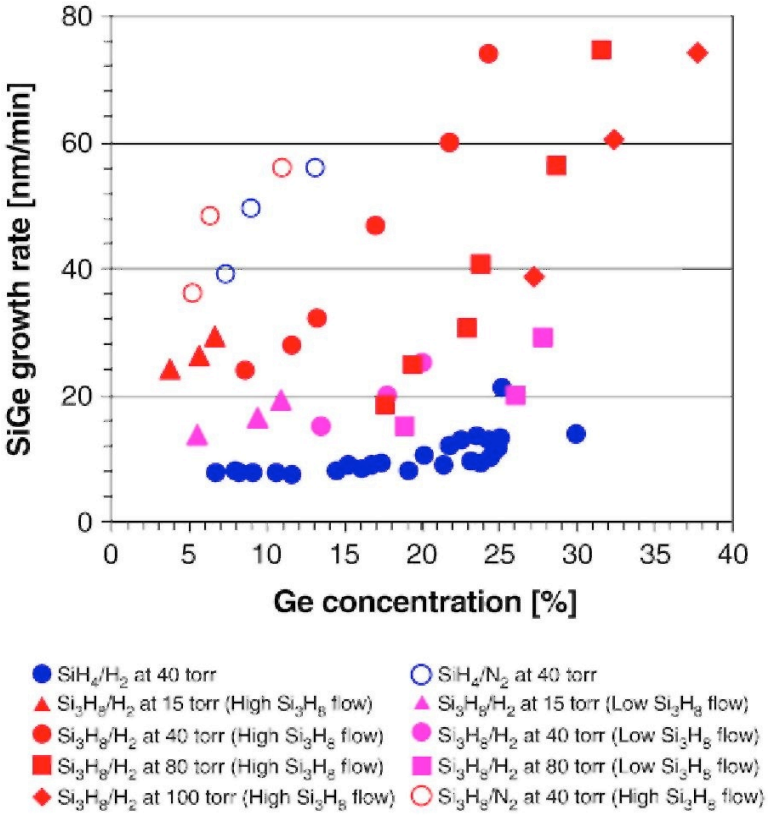

Published in: Thin Solid Film (2010); vol. 518; pp. S18-S22
Authors : Shotaro Takeuchi, Ngoc Duy Nguyen, Jozefien Goosens, Matty Caymax, Roger Loo
Statu : Postprint (Author's version)

Fig. *6. $Si_{1\_x}Ge_x$ growth rates using Si_3H_8/H_2 process with (a) C and (b) B doping, respectively. For comparison, the data of SiH_4/H_2 process was also shown. All $Si_{1-x}Ge_x$ layers were grown at 600 °C and 40Torr. For (a), blue symbols show SiH_4/H_2 process (Ge: 13%). Others show Si_3H_8/H_2 processes with high Si_3H_8 and GeH_4 flows (square) (Ge: 15%), low Si_3H_8 and high GeH_4 flows (triangle) (Ge: 20%), and high Si_3H_8 and low GeH_4 flows (diamond) (Ge: 6%). For (b), blue symbols show SiH_4/H_2 process (Ge: 13%), and red ones show high Si_3H_8 and GeH_4 flows (Ge: 15%).*

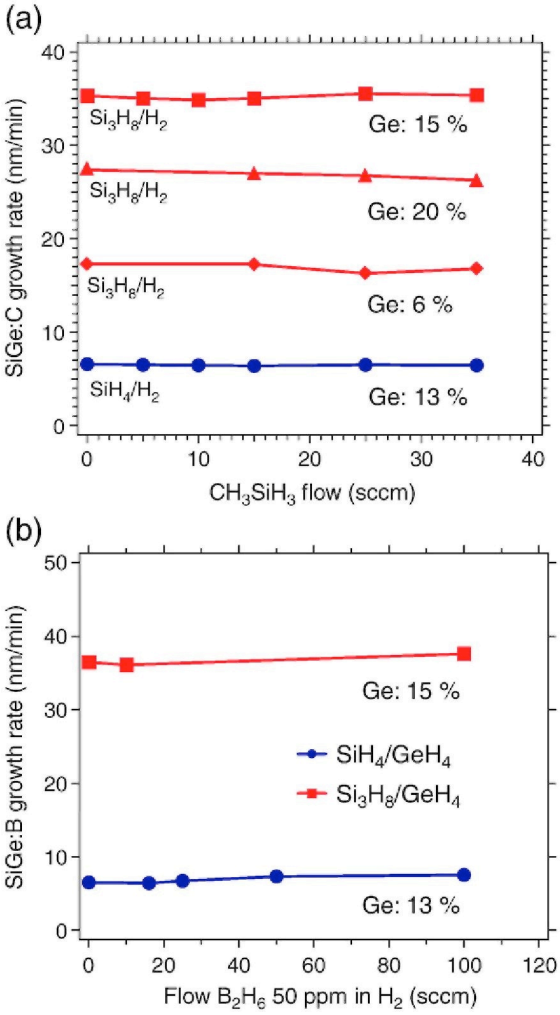

3.3. Boron- and carbon-doped $Si_{1-x}Ge_x$ *growth using* Si_3H_8/H_2 *process*

We have also demonstrated *in-situ* C- and B-doped $Si_{1-x}Ge_x$ growth using Si_3H_8/H_2 process for SiGe-based BiCMOS applications. Fig. 6(a) and (b) shows $Si_{1-x}Ge_x$ growth rates using Si_3H_8/H_2 process with B and C doping, respectively. For comparison, the data of SiH_4/H_2 process was also shown in Fig. 6. No significant impact of doping on growth rate in both doping cases was observed. For a similar Ge concentration, the use of Si_3H_8/H_2 gives 5 times higher growth rate than that of SiH_4/H_2. As shown in Fig. 7(a), total and active B concentration in both Si precursor gas cases increase with increasing effective B_2H_6 flow ranging from 10 to 100 seem. It should noted that the B dopant activation in the $Si_{0.85}Ge_{0.15}$ layer using the Si_3H_8/H_2 process is 34% higher than that with the SiH_4/H_2 process as shown in Fig. 7(b). This result indicates that the formation of electrically inactive B clusters can be avoided because the Si_3H_8/H_2 process is low thermal budget. Fig. 8 shows a SIMS profile of preliminary fabricated HBT base stacks using Si_3H_8/H_2 process, which includes a B dopant spike and a two-step Ge profile with C doping to reduce B diffusion. The B dopant spike layer with high B concentration of 1E20 at/cm^3 is well confined between C-doped $Si_{0.8}Ge_{0.2}$ layers.

4. Conclusions

We have demonstrated $Si_{1-x}Ge_x$ growth using Si_3H_8 as Si precursor gas and described the growth behavior. The $Si_{1-x}Ge_x$ growth using Si_3H_8/H_2 is a very efficient process with high crystalline layer quality and a high growth rate up to 74 nm/min. The obtained growth rates with Si_3H_8/H_2 are between 1.5 and 6 times higher than for SiH_4/

H_2 at a given growth condition. Our Si_3H_8-based $Si_{1-x}Ge_x$ process scheme leads to an improvement of the throughput and a reduction of the thermal budget, which is important especially for advanced BiCMOS applications. For advanced SiGe-based CMOS applications, high Ge concentrations are needed. At the moment, we can reach Ge concentration up to 40% with our Si_3H_8-based $Si_{1-x}Ge_x$ process. However, we expect that higher Ge concentrations are achievable by further optimization of the epitaxial growth conditions. This future investigation is a natural extension of the present work.

Fig. *7. (a) Total and active B concentrations in Sio.s5Geo.15 layer using Si_3H_8/H_2 process and (b) ratio of the active B concentration over the total B concentration as a function of the effective B_2H_6 flow. For comparison, the data obtained for the SiH_4/H_2 process are also shown. Red and blue symbols indicate Si_3H_8/H_2 and SiH_4/H_2 processes, respectively.*

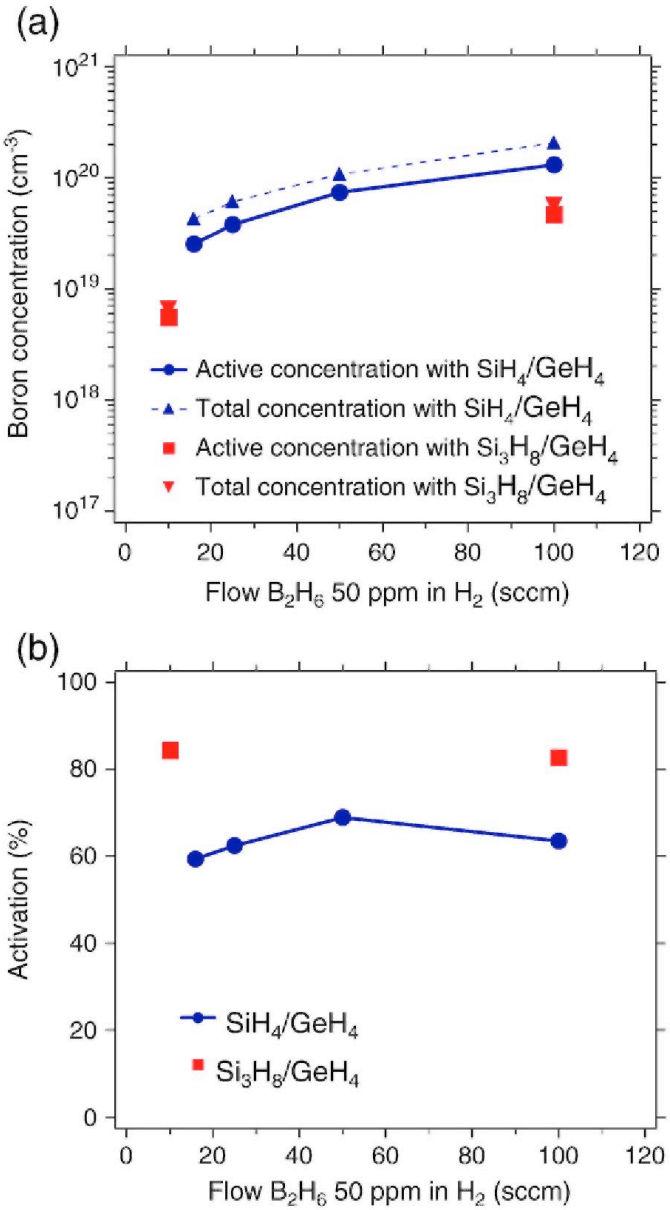

Fig. *8. Preliminary SIMS profiles of a preliminary fabricated HBT base stack using the Si_3H_8/H_2 process, which includes a B dopant spike and a two-step Ge profile with C doping to reduce B diffusion. B depth profile was measured by O^+ beam with a beam energy of 500 eV. Si, Ge, and C depth profiles were measured by Cs^+ beam with a beam energy of 5 keV. The C background level can be observed from about 50 nm, after the surface peak.*

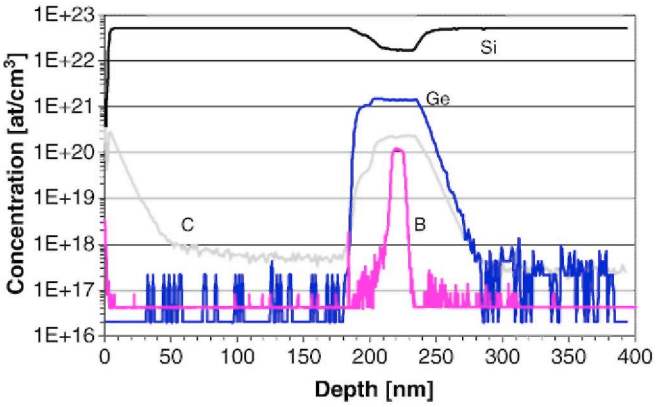

Acknowledgement

The supply of Silcore® by Voltaix, Inc. is gratefully acknowledged. The authors wish to thank Matthew Stephens and Michael Pikulin from Voltaix for helpful discussions. Fruitful discussion with Rick Wise (Texas Instruments) is gratefully acknowledged.

References

[1] Y.C. Yeo, Semicond. Sci. Technol. 22 (2007) SI 117.

[2] P. Verheyen, G. Eneman, R Rooyackers, R Loo, L. Eeckout, D. Rondas, F. Leys, J. Snow, D. Shamiryan, M. Demand, T.H.Y. Hoffmann, M. Goodwin, H. Fujimoto, C. Ravit, B.-C Lee, M. Caymax, K. De Meyer, P. Absil, M. Jurczalk, S. Biesemans, IEDM, technical digest, 2005, p. 907.

[3] P. Verheyen, V. Machkaoutsan, M. Bauer, D. Weeks, C. Kerner, F. Clemente, H. Bender, D. Shamiryan, R Loo, T. Hoffmann, P. Absil, S. Biesemans, S.G. Thomas, IEEE Electron Device Lett. 29 (2008) 1206.

[4] LJ. Choi, A. Sibaja-Hernandez, R Venegas, S. Van Huylenbroeclk, S. Decoutere, IEEE Trans. Electron Devices 55 (2008) 358.

[5] Y. Shimamune, M. Fukuda, M. Koiizuka, A Katakami, A Hatada, K. Ikeda, Y Kim, K. Kawamura, N. Tamura, T. Mori, A Moriya, Y Hashiba, Y. Inokuchi, Y Kunii, M. Kase, VLSI Tech. Dig. 116(2007).

[6] R Loo, A Hikavyy, F. Leys, M. Wada, K. Sano, B. De Vos, A. Pacco, M. Bargallo Gonzalez, E. Simoen, P. Verheyen, W. Vangerle, M. Caymax, Solid State Phenomena 145-146 (2009) 177.

[7] P. Meunier-Beillard, M. Caymax, K.V. Nieuwenhuysen, G. Doumen, B. Brijs, M. Hopstaken, L Geenen, W. Vandervorst, Appl. Surf. Sci. 224 (2004) 31.

[8] M.A Todd, K.D. Weeks, Appl. Surf. Sci. 224 (2004) 41.

[9] A Gouyé, O. Kermarrec, Y Campidelli, P. Bajolet, P. Tomasini, S.G. Thomas, T. Billon, D. Bensahel, *Abstracts of Int. Conf. Silicon Epitaxy and Heterostructures,* 2007, p. 204.

[10] N.D. Nguyen, R Loo, M. Caymax, Appl. Surf. Sci. 254 (2008) 6072.

[11] M.V. Fischetti, S.E. Laux, J. Appl. Phys. 80 (1996) 2234.

[12] P.M. Garone, J.C. Sturm, P.V. Schwartz, S.A Schwarz, B.J. Wilkens, Appl. Phys. Lett. 56 (1990) 1275.

[13] S.M. Gates, Surf. Sci. 195 (1988) 307.

[14] M. Stephens, Voltaix, U.S.A, private commun, Apr. 22, 2008.

[15] J.J. Watlkins, M.D. Sefcik, M.A. Rind, Inorg. Chem. 11 (1972) 3147.

[16] M. Caymax, F. Leys, J. Mitard, K. Martens, L Yang, G. Pourtois, W. Vandervorst, M. Meuris, and R Loo, submitted to *I. Electrochem. Soc.*